Supporting Information

Deciphering the mechanism and structural features of polysorbate 80 during adsorption on PLGA nanoparticles by attenuated total reflectance - Fourier transform infrared spectroscopy

Abhayraj S. Joshi, Avinash Gahane, Ashwani K. Thakur*

Department of Biological Sciences and Bioengineering, Indian Institute of Technology, Kanpur, Uttar Pradesh, India – 208016

*Corresponding author:

Ashwani K. Thakur,

Associate Professor,

Department of Biological Sciences and Bioengineering,

Indian Institute of Technology, Kanpur, Uttar Pradesh, India – 208016

Email id: akthakur@iitk.ac.in

Tel: +91-512-259-4077

Fax: +91-512-259-4010

CONTENTS:

1. Methods

   a. SM1 (Dynamic light scattering and Scanning electron microscopy)

   b. SM2 (Fourier transform infrared spectroscopy)

   c. SM3 (XPS characterization)

   d. SM4 (PVA determination)

   e. SM5a (Adsorption isotherm modeling)

   f. SM5b (Adsorption kinetic modeling)

   g. SM6 (Statistical analysis)

2. Calculations

   a. SC1 (Normalization of peak areas of polysorbate 80 using sodium azide standard)

   b. SC2 (Calculations for adsorption isotherm)

3. Tables

   a. Table S1 (Dilutions for preparation of standard curve of polysorbate 80)

   b. Table S2 (IR band assignment for polysorbate 80)

   c. Table S3 (DLS study of uncoated and coated nanoparticles)

   d. Table S4 (Adsorption data at different starting concentrations of polysorbate 80)

   e. Table S5 (Adsorption isotherm modeling: Parameters and interpretation)

   f. Table S6 (Measurement parameter for ATR-FTIR method)

   g. Table S7 (Mixture contents for surfactant coating procedure)

   h. Table S8 (XPS peaks and respective binding energies)

4. Figures

   a. S1 (Standard curve for polysorbate 80 in dry state)

   b. S2 (FTIR spectra of various dilution of polysorbate 80 in dry state)

   c. S3 (FTIR spectra of various dilution of polysorbate 80 in liquid state)

   d. S4 (FTIR spectra of various controls used in experiment)

e. S5 (Accuracy of ATR-FTIR method)

f. S6 (Scanning electron microscopy images of uncoated and polysorbate 80 coated PLGA nanoparticles)

g. S7 (FTIR spectra of uncoated and polysorbate 80 coated nanoparticles)

h. S8 (Elovich model)

i. S9 (Weber-Morris model)

j. S10 Part A (XPS spectra of uncoated and polysorbate 80 coated nanoparticles for 0.5-7.5 mg/ml concentrations)

k. S10 Part B (XPS spectra of uncoated and polysorbate 80 coated nanoparticles for 10-30 mg/ml concentrations + Binding energy and % atomic composition graphs)

l. S11 (Band shifts in real-time FTIR analysis for polysorbate 80 in presence of PLGA nanoparticles)

m. S12 Part A (Real-time FTIR analysis for polysorbate 80 alone)

n. S12 Part B (Real-time FTIR analysis for polysorbate 80 alone)

o. S13 (Standard curve for PVA)

5. References

METHODS:

SM1. Dynamic light scattering (DLS) and Scanning electron microscopy (SEM) –

The size, polydispersity index (PDI) and zeta potential of coated nanoparticles were determined using Malvern Zetasizer (Nano ZS90, Malvern Instruments Ltd., Malvern, Worcestershire, UK). The particle size is reported as intensity weighted hydrodynamic diameter whereas zeta potential is reported as per Smoluchowski's approximation[1, 2]. To avoid high concentration related excessive light scattering, 50 µl nanoparticle suspension was diluted 20 times to final volume of 1000 µl. Size and zeta potential were determined using glass cuvette and folded capillary cells, respectively. Uncoated nanoparticles processed with similar protocol of washing and centrifugation cycles were used as control.

The uncoated and coated nanoparticle samples were diluted 50-100 times. Of it, 5-10 µl sample was placed on glass coverslip attached to a copper stub with double sided carbon conductive tape. The samples were dried and coated using gold–palladium sputter coater (SC7620 Mini sputter coater, Quorum Technologies Ashford, Kent, UK, 18 mA current, 180 s). Gold coated nanoparticles were observed using NovaNano field emission microscope (FEI, Part of Thermo Fisher Scientific, USA) at different magnifications.

SM2. Fourier transform infrared (FTIR) spectroscopy –

It was performed using Bruker Tensor 27 IR spectrometer (Bruker Optik GmBH, Ettlingen, Germany) equipped with liquid nitrogen-cooled mercury-cadmium-telluride (MCT) detector and PIKE MIRacle ATR accessory under continuous purging with nitrogen gas. The method parameters were set as given in Table S6. The analysis was performed in two ways as follows.

First, to understand adsorption kinetics, polysorbate 80 samples separated from nanoparticles as per scheme 1 were used. 1 µL of each sample that is premixed with internal standard was put on zinc-selenide (ZnSe) crystal of ATR unit. For each sample, total 60 scans were recorded in the range of 4000-850 cm^{-1} with a resolution of 4 cm^{-1}. Spectrum of water was taken as background for all scans. Water compensation program (Opus software, Build 7.2, Bruker Optik GmBH, Ettlingen, Germany) was applied during every scan

in order to reduce effect of moisture. The spectrum gets automatically saved in the form of three data blocks namely; absorbance, sample interferogram and reference interferogram (Opus software, Build 7.2, Bruker Optik GmBH, Ettlingen, Germany). Atmospheric compensation program was used as post-FTIR data treatment for every sample to nullify the effect of CO_2 present in the surrounding environment. Data was saved in 'data-point' format (.dpt file). Remaining data treatment and calculations were done using Opus software.

Secondly, to understand the behavior of polysorbate 80 molecules after coming in contact with PLGA nanoparticles, we used repeated measurement mode which enabled us to get real-time scans of polysorbate 80 solutions when mixed with nanoparticle suspension. For this experiment water was used for recording background scan. 50 µl nanoparticle suspension was kept on ZnSe crystal of ATR unit. The number of scans per analysis was set to 16 and the analysis was done after every 30 seconds for a period of 10 minutes (*i.e*. total 20 scans after every 30 seconds). Remaining parameters were kept same as per table S6. In the next step, 50 µl of 0.1 mg/ml polysorbate 80 solution was mixed with the nanoparticle suspension which is already present on the crystal. Here, the final concentrations of polysorbate 80 and PLGA nanoparticles reduce by half of original concentration. The spectra were recorded as mentioned above. As the concentration of nanoparticles reduces by 50%, the absorption multiplier factor of 2 was applied for further calculations using 'Spectrum calculator program' (Opus software, Build 7.2, Bruker Optik GmBH, Ettlingen, Germany). The spectra of nanoparticles were subtracted from that of nanoparticle-surfactant mixture by using 'Spectrum subtraction program' (Opus software, Build 7.2, Bruker Optik GmBH, Ettlingen, Germany). This yields the spectra of polysorbate 80 solution. Second derivative spectra were calculated using Origin Pro 9.1.0 (64 bit, Sr3, b275, OriginLab Corporation, Northampton, MA01060, USA) with 15 smoothening points to get resolved peaks. Spectrum of each minute (0 to 9 minute – total 10 spectra) was presented in stacked format to observe shifts of IR bands, if there are any. Same experiment was repeated for remaining concentrations.

SM3. X-ray photoelectron spectroscopy (XPS) for surface characterization –

The uncoated and polysorbate 80 coated nanoparticles were lyophilized and approximately 2-4 mg lyophilized powder was put on aluminum stage using conductive carbon tape. XPS was performed using PHI 5000 Versa Probe II, FEI Inc., Germany in vacuum (10^{-7} Pa). Initially single broad scans were performed for all samples at pass energy of 187.85 eV with step of 0.8 eV in the range of 0-1100 eV. X-ray was set at default setting (100u25W15kV). In order to achieve greater accuracy, narrow scans were performed (10 cycles per sample) at pass energy of 23.50 eV with step of 0.05 eV. Each narrow scan was performed in the range of 278-298 eV for carbon (C, 1s) as well as 523-548 eV for oxygen (O, 1s). The analysis time for single sample varied from 2.3-2.6 min for broad scan and 50-60 min for narrow scan. The data files obtained after XPS scans (*.vms format) were opened in Avantage Surface Chemical Analysis software (Version 5.962, Demo license, Thermo-Fisher Scientific Ltd.). First using 'User background' option (Modify menu), 'Smart background' was added to selected XPS data. Then, the calibration was done by correcting binding energy (BE) scale (Analysis menu) to 284.8 eV which represents C-C bond. Finally, deconvolution was carried out by adding four peaks which represent four different functionalities (Peak fitting menu) (Table S8) (Please see results and discussion section). After using default fit options (100 iterations, 'Powel' fitting algorithm and 'Gaussian-Laurentz' mixed peaks product) added peaks were fitted. Chi-square value, Abbe criterion, binding energy (BE) corresponding to peak maxima and percent atomic constitution was noted down. Graph of 'Counts/seconds' versus BE was plotted to show original data, fitted peaks and fit cumulative.

SM4. Determination of amount of PVA by UV-Visible spectrophotometric method –

Separated PVA (Scheme 1, Step D) was first dried using vacuum desiccator to remove residual content of acetonitrile which was used for its precipitation. After drying, 100 µl water was added to dissolve PVA pellet. PVA quantification was done using E. Allemann's method[2-4]. Briefly, to 100 µl PVA solution, 10 µl iodine solution [iodine (0.05 M): potassium iodide (0.15 M)] and 50 µl boric acid solution (0.65 M) were added. Final volume was made

to 500 µl with water. All samples were then analyzed using multiplate reader (BioTek Synergy H4 Hybrid Reader, BioTek, USA) at 690 nm. Standard curve (Figure S13) obtained from various dilutions of 30 mg/ml aqueous solution of PVA was used to calculate the amount of PVA in each sample.

SM5a. Adsorption isotherm modelling[5] –

Several adsorption isotherm models are available for determining the probable adsorption mechanism of an adsorbate on a solid surface under given set of experimental conditions. Among all the models, we first applied two basic empirical models; Langmuir isotherm model and Freundlich isotherm model. These two models were used for deciphering whether polysorbate 80 follows monolayer or multilayer adsorption pattern. It has been proved that various surfactants exhibit molecular interactions with colloidal surfaces while being adsorbed[6, 7]. But Langmuir or Freundlich model do not assume existence of such interactions. Hence, we applied Temkin model which gives idea about presence or absence of repulsive interactions among adorbate molecules[8]. It also considers heterogeneity of surface unlike Langmuir model. Temkin isotherm gives value of heat of adsorption which generally decreases as surface coverage increases. On the other hand Flory-Huggins model considers inter-molecular interactions of adsorbate and adsorbent molecules[5, 9, 10]. Also, the Gibb's free energy can be calculated using this model. Using the value of Gibb's free energy, the process can be identified as either physisorption or chemisorption. No single model can give perfect description of probable mechanism[5]. Hence using these three adsorption isotherm models, we have speculated the mechanism of polysorbate 80 adsorption. From FTIR data, we obtained the adsorbed amount of surfactant on PLGA nanoparticles (Q_e). Using following equation, we first calculated concentration of surfactant in bulk liquid at the time of equilibration (C_e).

$$Q_e = \frac{(C_0 - C_e)V}{m} \tag{1}$$

a. Langmuir isotherm model is represented as,

$$Q_e = \frac{Q_0 b C_e}{1 + b C_e} \tag{2}$$

The linear form of this equation is,

$$\frac{C_e}{Q_e} = \frac{1}{bQ_0} + \frac{C_e}{Q_0}$$

(3)

The graph of C_e/Q_e versus C_e yields a straight line with the slope equals to $1/Q_0$ and an intercept equals to $1/bQ_0$. Once we get values of Q_0 and b, we can calculate a dimensionless factor, commonly known as separation factor– R_L by the following equation

$$R_L = \frac{1}{1 + bC_0}$$

(4)

This factor has limits as given below based on which interpretation can be done[5, 11].

$R_L > 1$ →   Unfavorable adsorption process
$R_L = 1$ →   Linear process
$0 < R_L < 1$ → Favorable adsorption process
$R_L = 0$ →   Irreversible adsorption

b. Freundlich isotherm model is represented by the following equation,

$$Q_e = K_f C_e^{1/n}$$

(5)

The linear form of this equation is,

$$Log\ Q_e = Log\ K_f + \frac{1}{n} Log\ C_e$$

(6)

The graph of Log Q_e versus Log C_e yields a straight line with the slope of $1/n$ and an intercept of Log K_f. The value of $1/n$ between 0 and 1 represent heterogeneous adsorption[5].

c. Temkin isotherm model[8] is represented by,

$$Q_e = \frac{RT}{b_t} \ln A_t C_e$$

(7)

The linear form of this equation is,

$$Q_e = \frac{RT}{b_t} \ln A_t + \frac{RT}{b_t} \ln C_e$$

(8)

The graph of Q_e versus $ln(C_e)$ yields a straight line with the slope of (RT/b_t) and an intercept of $(RT/b_t).ln(A_t)$. From slope of graph, b_t i.e. heat of sorption can be calculated in terms of KJ/Mol. If the heat of adsorption is below 40 KJ/Mol then the process is physical adsorption (Physisorption) and if the value lies between 40-200 KJ/Mol then it is termed as chemical adsorption (Chemisorption)[12].

d. Flory-Huggins model[5, 9, 10] is represented by,

$$\frac{\theta}{C_0} = K_{fh}(1-\theta)^{n_{fh}} \qquad (9)$$

The linear form of this equation is,

$$Log\left(\frac{\theta}{C_0}\right) = Log\,K_{fh} + n_{fh}Log(1-\theta) \qquad (10)$$

The value of surface coverage (θ) can be calculated as $(1-C_e/C_0)$. The graph of $Log(\theta/C_0)$ versus $Log(1-\theta)$ yields a straight line with the slope of n_{fh} and an intercept of $Log\,K_{fh}$. From the intercept, Gibb's free energy can be calculated by following equation,

$$\Delta G = -RTlnK_{fh} \qquad (11)$$

Glossary:

Term	Meaning
Q_e	Amount adsorbed on nanoparticles at equilibrium (µg/mg)
C_0	Concentration of surfactant at the start of experiment in bulk liquid (µg/ml)
C_e	Concentration of surfactant at the equilibrium in bulk liquid (µg/ml)
V	Total volume of surfactant solution in which nanoparticles were incubated (ml)
m	Total mass of nanoparticles incubated with surfactant solution (mg)
Q_0	Maximum monolayer coverage capacity according to Langmuir adsorption isotherm (µg/mg)
b	Langmuir isotherm constant
R_L	Separation factor calculated from Langmuir adsorption isotherm
K_f	Freundlich isotherm constant related to adsorption capacity of adsorbent
n	Adsorption intensity calculated from Freundlich adsorption isotherm
R	Universal gas constant (8.314 J/Mol.K)
T	Temperature (Kelvin)
A_t	Temkin isotherm equilibrium binding constant (ml/µg)
b_t	Temkin isotherm constant
θ	The degree of surface coverage
K_{fh}	Flory-Huggins isotherm equilibrium constant (ml/µg)
n_{fh}	Flory-Huggins isotherm model exponent
Q_t	Amount of surfactant adsorbed per mg of nanoparticles at time 't'
t	Time
t_{eq}	Time at which equilibrium point in adsorption kinetics was achieved
t_0	Start time for adsorption process
α	Initial adsorption rate according to Elovich model of adsorption kinetics
a	Desorption constant according to Elovich model of adsorption kinetics
k_{int}	Intraparticle diffusion rate constant according to Weber-Morris model of adsorption kinetics
δ	Intercept in graph of Weber-Morris model of adsorption kinetics representing boundary layer effect

SM5b. Adsorption kinetic modelling[13] –

a. <u>Elovich model</u> = This model was initially developed for analyzing the adsorption of gases on solid surfaces. Elovich model is applied to adsorption where adsorbate-adsorbent interact chemically at molecular level. The adsorption process involving heterogeneous surface and chemisorption process often follow Elovich model. To confirm the physisorption process of polysorbate 80 on PLGA nanoparticles, we used Elovich model as negative control. The Elovich model is represented as,

$$\frac{dQ}{dt} = \alpha e^{-\alpha Q} \qquad (9)$$

The linear form of above equation is,

$$Q_t = \alpha \ln(a.\alpha) + \alpha \ln(t) \qquad (10)$$

Thus, graph of Q_t versus ln (t) will yield straight line with the slope of α and an intercept of $\alpha.ln$ (aα).

b. <u>Weber-Morris model</u> = This model states the process of transfer of adsorbate molecules from bulk liquid to the solid surface. The diffusion of adsorbate molecules from liquid to adsorbent surface is driven by concentration gradient[8]. However, once reached to the surface, the solvent molecules associated with surface (film) and porous nature of surface (intraparticle spaces) affect the adsorption process. Thus diffusion through film or intraparticle spaces or both represent limiting step of adsorption. Weber-Morris model is represented by,

$$Q_t = k_{int}t^{1/2} \qquad (11)$$

Thus, the plot of Q_t versus $t^{1/2}$ yields a straight line with the slope of k_{int}. The Weber-Morris model is generally represented as given in equation (11), however same equation along with an intercept can also be found in the literature[11, 14].

$$Q_t = k_{int}t^{1/2} + \delta \qquad (12)$$

where, δ represents the boundary layer effect

Higher is the value of the intercept, larger will be the boundary layer effect. Hence, the interpretation is done with respect to the line obtained by eq. (12). If the line is passing

through the origin then intraparticular diffusion is said to be the *'only'* rate limiting step in adsorption kinetics. But in many cases of adsorption studies, an intercept exists suggesting possibility of boundary layer effect[11]. Boundary layer is the representation of accumulation of solvent molecules around the solid adsorbent particle. In case of PLGA nanoparticles, we believe, water molecules and PVA molecules may present as boundary for polysorbate 80 molecules. If the line is not passing through the origin and the graph shows multiple linear regions, then the adsorption kinetics consists of multiple mechanisms such as initial rapid diffusion of adsorbate from bulk liquid to solid surface, penetration of molecules through the boundary layer surrounding the solid surface and finally intraparticulate diffusion in the surface of solid adsorbent. In this case, all steps contribute to the overall rate of adsorption.

SM6. Statistical analysis –

All experiments were done in triplicate. The data is represented as mean±standard deviation for all experiments. Statistical analysis was performed using Sigmaplot software at confidence interval of 95% (level of significant 0.05). *t*-test was applied to check significance among time points in adsorption curve. Same test was used for analyzing DLS data and PVA quantification data. Observations showing P-value lesser than level of significance (0.05) were considered differing significantly from each other. Regressional analysis was performed for adsorption isotherms using Origin Pro software (linear fit function) and based on goodness of fit (r^2 value), inferences were drawn. In case of IR signature bands of samples, significant difference was determined on the basis of resolution fixed for ATR-FTIR method (4 cm^{-1}). Band shifts higher than 4 cm^{-1} were considered to be significant.

CALCULATIONS:

SC1. Calculations for normalization of area during quantification of polysorbate 80 by ATR-FTIR method –

As mentioned in 'Methods' section, sodium azide was added as an internal standard for ATR-FTIR method. We selected fixed concentration of sodium azide (1 mg/ml) and 1 μl of this solution was added to 50 μl of polysorbate 80 sample. After analysis and integration of peaks, we got two areas; say '*x*' for polysorbate 80 and '*y*' for sodium azide. However, if we analyze same sample again, due to influence of environment, we may get variation in IR intensity. Let's say the intensity of overall spectra got reduced by 2. Thus, after integration, the peak areas for same sample will now be '*x*/2' and '*y*/2'. In this scenario, if we consider absolute areas then in calculations, we will have to consider the factor of 2. If calculations are done without this factor then erroneous data will be generated. Hence, to avoid this, we used the ratio of polysorbate 80 area to sodium azide area. Because of this method, the results of two different analysis will be same as follows…

$$\frac{x}{y} = \frac{x/2}{y/2}$$

Hence, the user will no longer need the multiplication factor and the calculations will be correct. We used same concentration and same amount of sodium azide in all the samples. Thus, the change in ratio will be due to change in polysorbate 80 concentration solely and not because of change in intensity. This makes polysorbate 80 quantification accurate in all the samples and also enables the user to obtain adsorption kinetics data.

SC2. Calculations for Langmuir adsorption isotherm analysis –

1. Langmuir model –

   Slope = 0.09, Intercept = 9.72

   ∴ Q_0 = 11.11, ∴ b = 0.0093

   Hence, R_L values for each concentration using equation (4). The values are given in table S4. All are within the range of 0-1. Hence, for all concentrations, the adsorption process is favorable. Also, as the starting concentration of polysorbate 80 increases, RL value

decreases exponentially which further confirms saturation zone of adsorption above 1 mg/ml concentration.

2. Flory-Huggins model –

   Intercept = (Log K_{fh}) = -6.90, $\therefore$ K_{fh} = 1.3000e-7

   According to the equation, ΔG=38.34 KJ/Mol.

   This value represents physisorption process.

SUPPORTING TABLES:

Table S1: Standard dilutions of polysorbate 80 used to prepare standard curve

Sample code	Amount of 0.5 mg/ml polysorbate 80 solution (µl) taken (equivalent µg of polysorbate 80)	Amount of water (µl)	Final volume (µl)	Final concentration of solution (µg/ml)	Amount of polysorbate 80 in 1µl sample analyzed by FTIR (ng)
A	1.25 (0.625)	1998.75	2000	0.3125	0.3125
B	2.5 (1.25)	1997.50	2000	0.625	0.625
C	5 (2.5)	1995	2000	1.25	1.25
D	10 (5)	1990	2000	2.5	2.5
E	20 (10)	1980	2000	5	5
F	30 (15)	1970	2000	7.5	7.5
G	40 (20)	1960	2000	10	10
H	60 (30)	1940	2000	15	15
GI	80 (40)	1920	2000	20	20

Table S2: IR band assignment for polysorbate 80

Sr. No.	IR band position [Peak maxima] (cm^{-1})	Interpretation
1.	3400-3200 [3260]	Water vapors (O-H group)
2.	3000-2800 [2925 and 2860]	-CH_2 group symmetric and asymmetric stretching vibrations (acyl chain of polysorbate 80)
3.	2195-2095 [2160]	Sodium azide peak (internal standard)
4.	1770-1720 [1740]	-C=O group vibrations (ester group of polysorbate 80)
5.	1690-1680 [1672]	-C=C group vibrations (alkene group of oleic acid part of polysorbate 80)
6.	1630-1580 [1593]	-C-C stretching vibration in a ring (sorbitan part of polysorbate 80)
7.	1500-1400 [1466]	-C-H band (acyl chain of polysorbate 80)
8.	1200-1050 [1110]	-C-O group vibrations (ethoxy group of polysorbate 80)

Table S3: DLS study of uncoated and coated nanoparticles at different starting concentrations of polysorbate 80

Batch	Size (d, nm) †	PDI†	Z.P. (mV) †	Q_e (µg/mg)
Uncoated	152.5 ± 2.1	0.021 ± 0.002	N.A.	N.A.
Coated (0.1 mg/ml)	155.8 ± 3.7	0.023 ± 0.015	-32.0 ± 1.6	4.6 ± 1.0
Coated (0.3 mg/ml)	150.2 ± 2.9	0.039 ± 0.010	-35.5 ± 1.2	5.7 ± 0.8
Coated (0.5 mg/ml)	150.2 ± 1.1	0.028 ± 0.020	-33.4 ± 1.9	10.6 ± 0.9
Coated (1 mg/ml)	151.7 ± 1.5	0.043 ± 0.040	-34.0 ± 1.7	10.6 ± 1.7
Coated (3 mg/ml)	147.5 ± 1.2	0.045 ± 0.039	-33.4 ± 4.4	10.8 ± 2.0
Coated (5 mg/ml)	152.5 ± 1.2	0.040 ± 0.037	-33.7 ± 3.5	9.4 ± 1.6
Coated (7.5 mg/ml)	148.7 ± 2.0	0.042 ± 0.040	-35.1 ± 1.6	9.8 ± 3.1
Coated (10 mg/ml)	150.6 ± 1.4	0.022 ± 0.016	-35.1 ± 1.6	8.8 ± 1.3
Coated (20 mg/ml)	150.6 ± 1.2	0.036 ± 0.016	-35.1 ± 1.6	11.5 ± 1.1
Coated (30 mg/ml)	149.8 ± 1.2	0.021 ± 0.010	-35.1 ± 1.6	10.2 ± 2.8
†All values at the time of equilibration.				
All values represented as mean ± standard deviation (n=3)				
d – Diameter of nanoparticles, Z.P. – Zeta potential, Q_e – Adsorbed amount				
N.A. – Not applicable				

Table S4: Adsorption data at different starting concentrations of polysorbate 80 (represented in Fig. 6 of manuscript)

Time (Min)	0.1 mg/ml Amount (µg per mg)			0.3 mg/ml Amount (µg per mg)			0.5 mg/ml Amount (µg per mg)			1 mg/ml Amount (µg per mg)			3 mg/ml Amount (µg per mg)		
	A	B	C	A	B	C	A	B	C	A	B	C	A	B	C
5	1.19	1.43	1.56	5.01	2.78	2.43	0.00	0.28	0.95	0.02	3.41	2.60	10.10	8.51	6.92
10	1.61	0.95	1.56	1.61	2.14	4.35	3.56	6.69	8.96	3.73	4.79	5.86	8.19	13.60	5.32
20	3.01	0.78	3.01	1.61	1.50	2.46	11.16	10.78	8.51	6.39	11.06	9.04	15.94	10.10	8.51
30	2.14	0.55	0.55	1.69	1.61	3.12	9.70	10.33	11.29	10.63	12.33	8.96	3.20	4.79	4.53
60	0.92	0.32	0.87	3.41	3.73	4.05	12.65	16.29	15.58	11.16	9.87	6.60	8.51	11.69	12.33
120	1.74	0.32	0.55	6.60	5.32	5.08	10.98	9.57	11.34	6.92	3.73	4.26	19.33	21.24	11.69
240	3.56	4.69	5.54	3.41	3.73	2.78	11.11	12.33	12.97	5.32	7.24	6.39	17.26	23.63	22.30

Time (Min)	5 mg/ml Amount (µg per mg)			7.5 mg/ml Amount (µg per mg)			10 mg/ml Amount (µg per mg)			20 mg/ml Amount (µg per mg)			30mg/ml Amount (µg per mg)		
	A	B	C	A	B	C	A	B	C	A	B	C	A	B	C
5	4.26	2.14	0.55	7.24	13.28	8.96	7.35	9.57	9.57	12.40	11.69	10.28	7.87	9.38	13.28
10	6.12	3.73	6.12	5.32	18.06	7.71	7.64	5.86	2.14	8.05	2.41	13.51	7.87	3.96	12.01
20	6.12	6.92	4.53	7.87	13.81	10.33	4.69	4.37	2.67	2.50	5.78	13.81	9.57	3.84	14.30
30	6.39	7.71	3.41	9.78	12.75	10.33	5.64	3.59	4.53	12.01	8.51	9.67	10.63	4.26	7.24
60	9.15	7.87	11.06	7.45	14.24	10.63	5.96	4.62	5.86	11.11	11.11	4.00	11.37	2.14	8.19
120	12.97	12.33	13.28	9.04	12.15	13.28	6.60	6.74	5.06	12.33	4.93	4.69	7.71	5.08	2.54
240	9.78	12.97	10.10	11.69	12.15	12.15	5.32	8.86	6.12	11.06	2.37	5.64	12.09	5.86	3.05

Table S5: Adsorption isotherm modeling: Parameters and interpretation

Adsorption isotherm model	Parameter	Value	Limits	Inference
Langmuir	Correlation coefficient (r^2)	0.9522	0-1	Best fit
	Slope ($1/Q_0$)	0.09	N.A.	
	Intercept ($1/bQ_0$)	9.72	N.A.	
	Maximum adsorption capacity (Q_0)	11.11	N.A.	
	b	0.0093	N.A.	

	R$_L$ value (From lower to higher starting concentration of polysorbate 80) (0.1 mg/ml to 30 mg/ml)	0.5181 0.2638 0.1770 0.0971 0.0346 0.0211 0.0141 0.0106 0.0053 0.0036	0-1	Favorable adsorption
Freundlich	Correlation coefficient (r^2)	0.3019	0-1	Poor correlation
Temkin	Correlation coefficient (r^2)	0.5388	0-1	Poor correlation
Flory-Huggins	Correlation coefficient	0.9109	0-1	Fairly good correlation
	Log K$_{fh}$	-6.90	N.A.	N.A.
	ΔG	38.34 kJ/Mol	Below 40	Physisorption

Table S6: Measurement parameters for FTIR method

Sr. No.	Parameter	Value
Group A (Advanced measurement)		
1	Resolution	4 cm^{-1}
2	Sample scan number	60
3	Background scan number	120
4	Save data from	4000-850 cm^{-1}
5	Result spectrum	Absorbance
6	Additional data treatment a	Water compensation program
7	Additional data treatment b	Atmospheric compensation program
8	Data blacks to be saved	a. Absorbance b. Single channel spectrum c. Reference channel spectrum
Group B (Optic)		
1	External synchronization	Off
2	Source setting	MIR
3	Beam splitter	KBr
4	Optical filter setting	Open
5	Aperture setting	2 mm
6	Accessary	ZnSe ATR unit
7	Detector setting	LN-MCT Photovoltaic detector
8	Scanner velocity	10 KHz
Group C (Acquisition)		
1	Wanted high frequency limit	8000
2	Wanted low frequency limit	0
3	Laser wavenumber Interferogram size FT Size	15798.19 148218 16 K
4	High pass filter	Open
5	Low pass filter	10 KHz
6	Acquisition mode	Double sided, forward-backward mode
7	Correlation mode	Off
8	External analog signals	Off
Group D (Fourier Transform [FT] parameters)		
1	Phase resolution	32
2	Phase interferogram points	1778
3	Phase correlation mode	Mertz
4	Apodization function	Blackman-Harris B-term
5	Zero-filling factor	2

Table S7: Mixture contents for surfactant coating procedure

Concentration of polysorbate 80 (mg/ml)	0 (Control)	0.1	0.3	0.5	1	3	5	7.5	10	20	30
Nanoparticle suspension (μl) (~ 2.36 mg PLGA NP)	1000	1000	1000	1000	1000	1000	1000	1000	1000	1000	1000
Polysorbate 80 stock solution (μl)	0	2.5*	7.5*	12.5*	25*	75*	125*	187.5*	62.5†	125†	187.5†
Water (μl)	250	247.5	242.5	237.5	225	175	125	62.5	187.5	125	62.5
Total volume (μl)	1250	1250	1250	1250	1250	1250	1250	1250	1250	1250	1250

*50 mg/ml Polysorbate 80 stock solution, †200 mg.ml polysorbate 80 stock solution

Table S8: XPS peaks and respective binding energies selected for deconvolution and peak fitting procedure

Binding energy (BE, eV)	Assigned functional groups
284	Carbon-Carbon single covalent bond (-C-C-)
285	Carbon-Oxygen bond involved in alcohols (-C-OH)
286	Carbon-Oxygen bond involved in ethoxy group, ester group and cyclic ether(-C-O-C-)
288	Carbon involved in carboxylic group (-COOH)

SUPPORTING FIGURES:
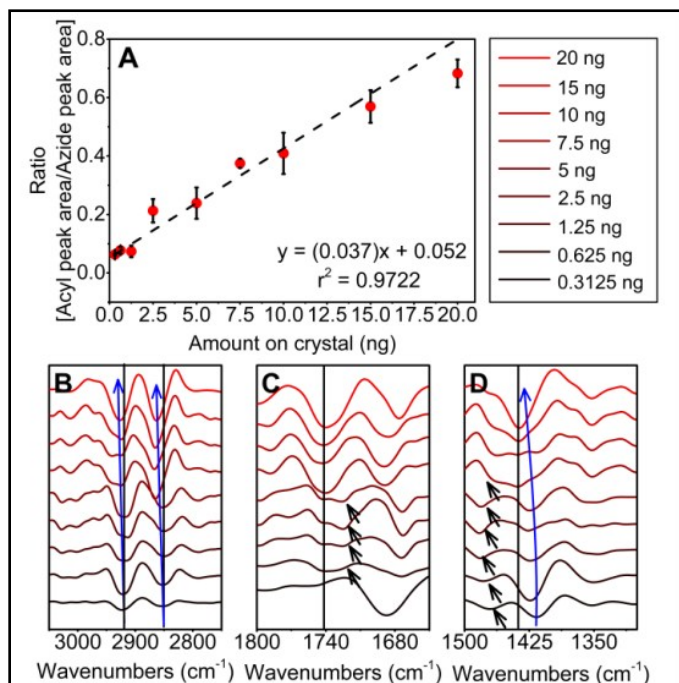
Figure S1: FTIR analysis of polysorbate 80 samples in dry state (1 μl sample air dried on ZnSe crystal). S1A represents the standard curve for various concentrations of polysorbate 80. Interestingly, depending on concentrations, band shifts (blue arrows) were observed for acyl chain stretching vibrations (B) and scissoring vibrations (D). In stretching vibrations of –C=O

group (C) and scissoring vibrations of acyl groups (D), peak fusion (black arrows) was also observed.
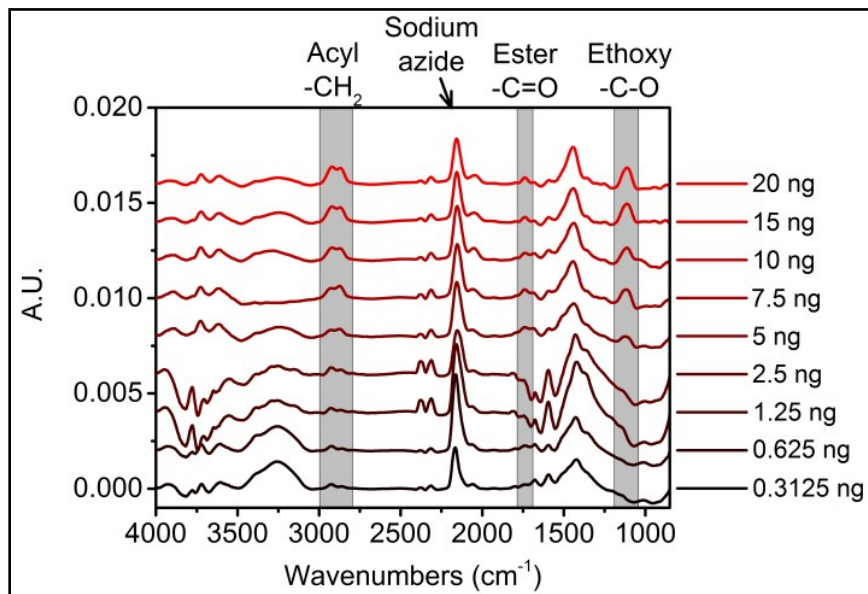
Figure S2: FTIR spectra of polysorbate 80 dilutions at different concentrations in dry state
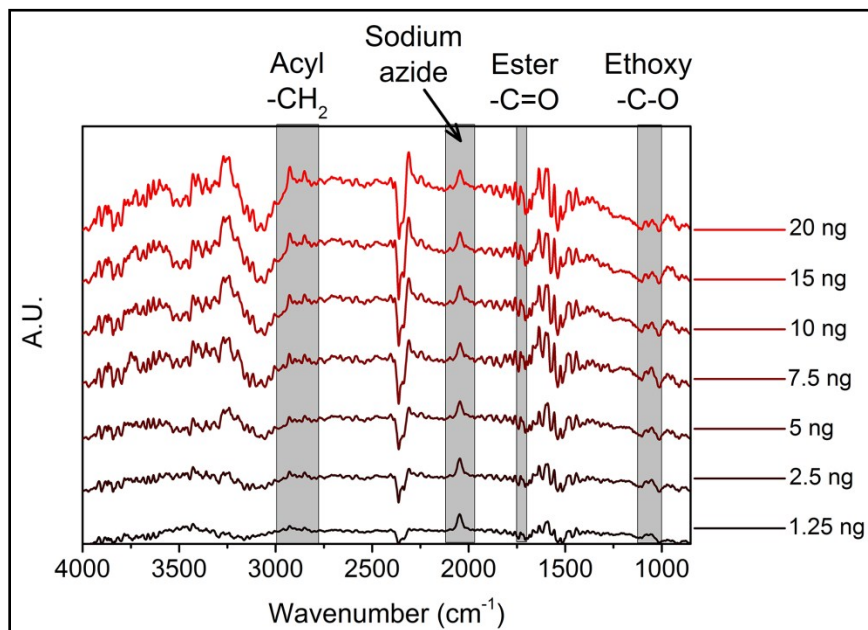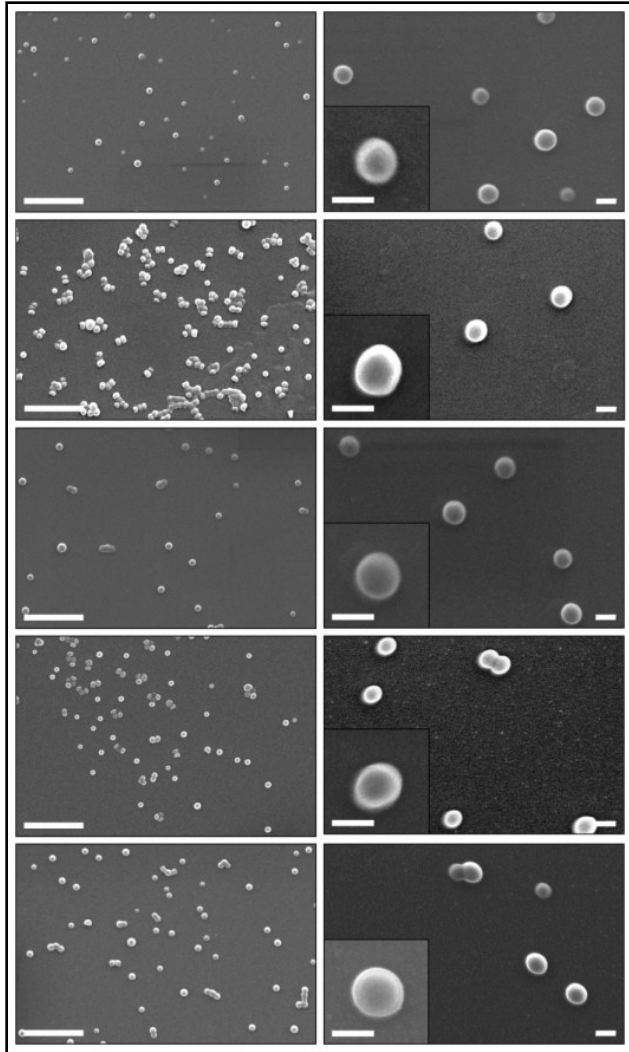

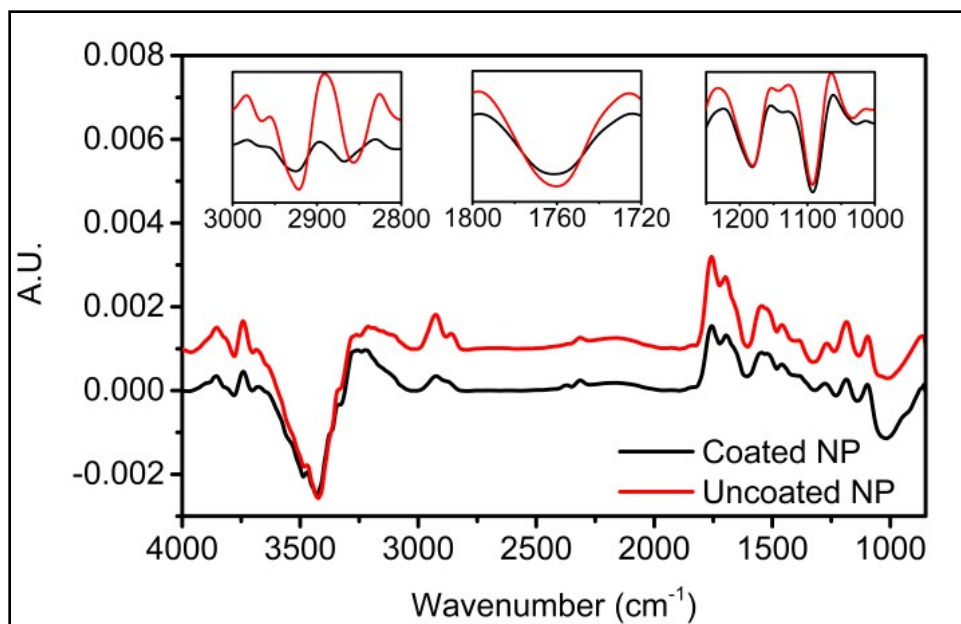**Figure S3:** FTIR spectra of polysorbate 80 dilutions at different concentration in liquid state
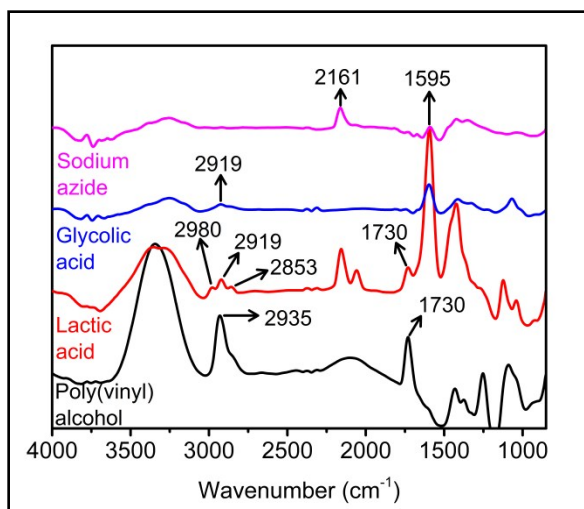
**Figure S4:** FTIR spectra of various control samples used in the experiment
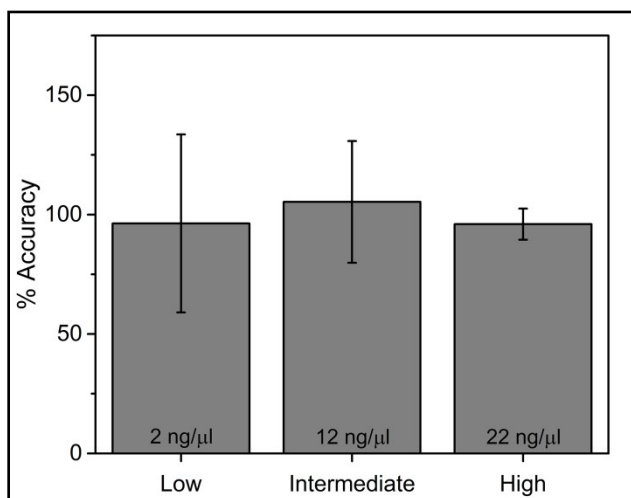
**Figure S5:** Percentage accuracy of ATR-FTIR method for polysorbate 80

Figure S6: Scanning electron microscopy (SEM) images of representative samples of PLGA nanoparticles (From top to bottom: Uncoated, 5 mg/ml coated, 10 mg/ml coated, 20 mg/ml coated and 30 mg/ml coated). The left and right columns show images captured at 15000X (Scale bar = 1 μm) and 50000X (Scale bar = 100 nm) magnification, respectively. The inset images (right column) of individual nanoparticles have been captured at 100000X magnification (Scale bar = 100 nm).

Figure S7: FTIR spectra of uncoated and polysorbate 80 coated PLGA nanoparticles. The signature peaks of polysorbate 80 (Acyl chain $-CH_2$ peak, ester $-C=O$ and ethoxy $-C-O$ peaks) could not be distinguished even in second derivative spectra (inset, three graphs) and thus extraction strategy was applied in order to separate polysorbate 80 from nanoparticles.
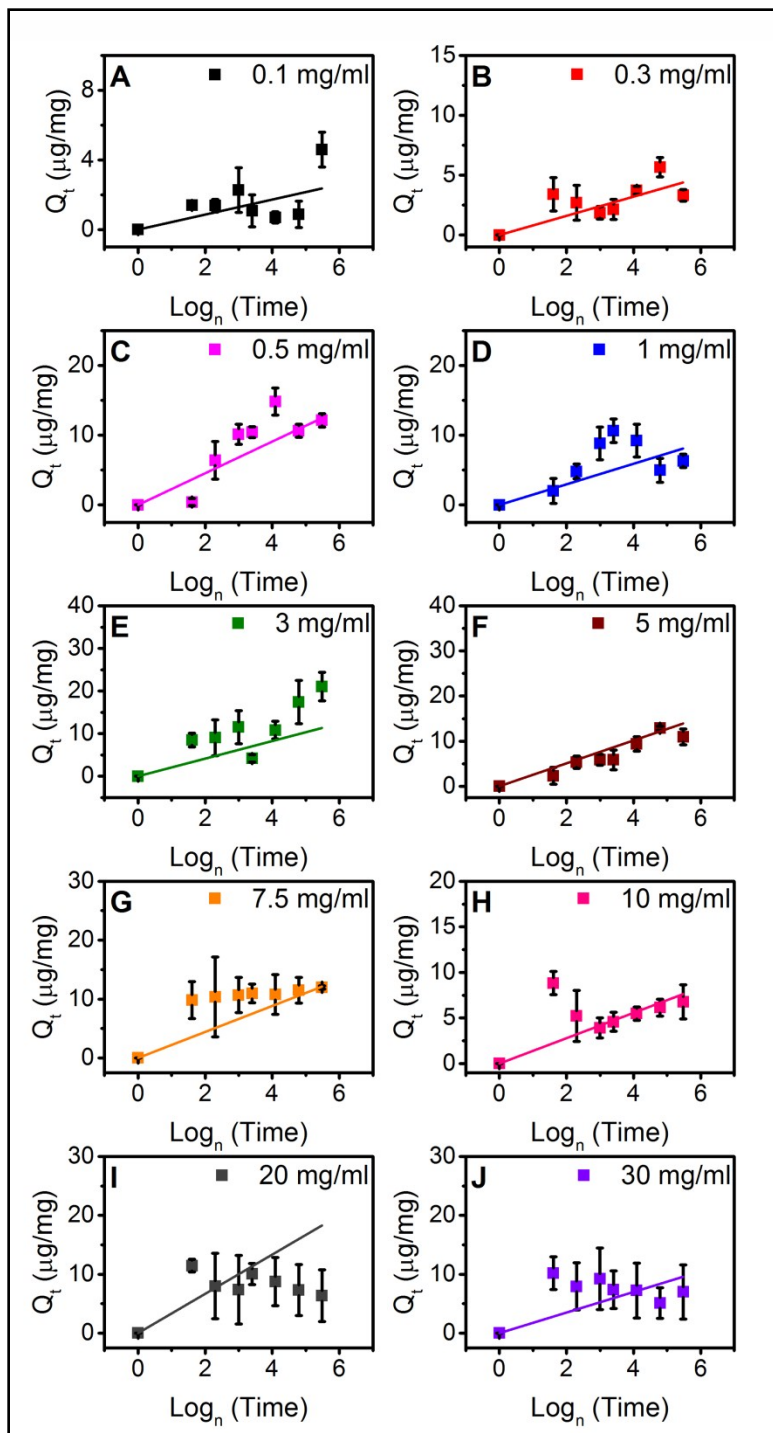
**Figure S8:** Elovich model applied to adsorption data.
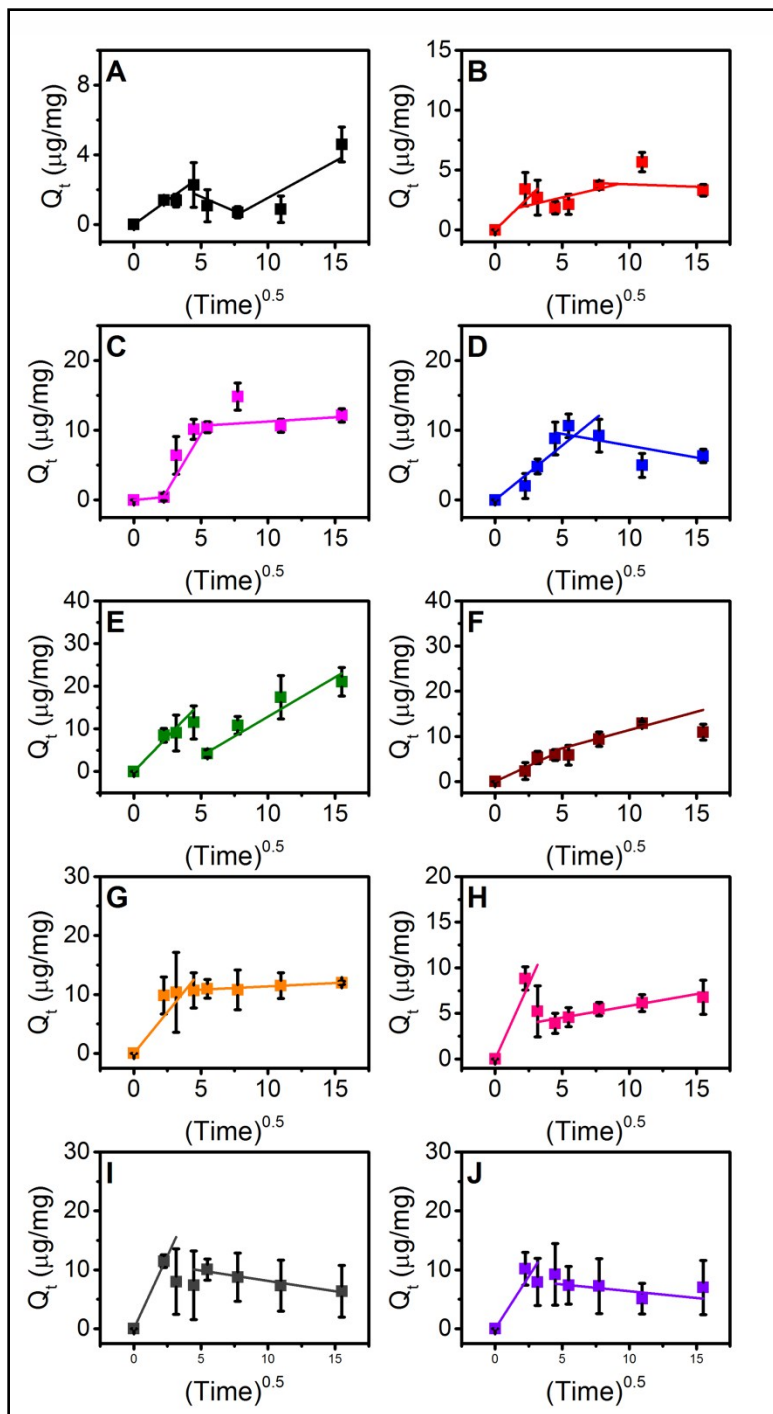
Figure S9: Weber-Morris model applied to adsorption data showing multiple linear regions. No line passes through the origin which suggests that the adsorption process consist of multiple steps and all steps contribute to overall rate of adsorption.
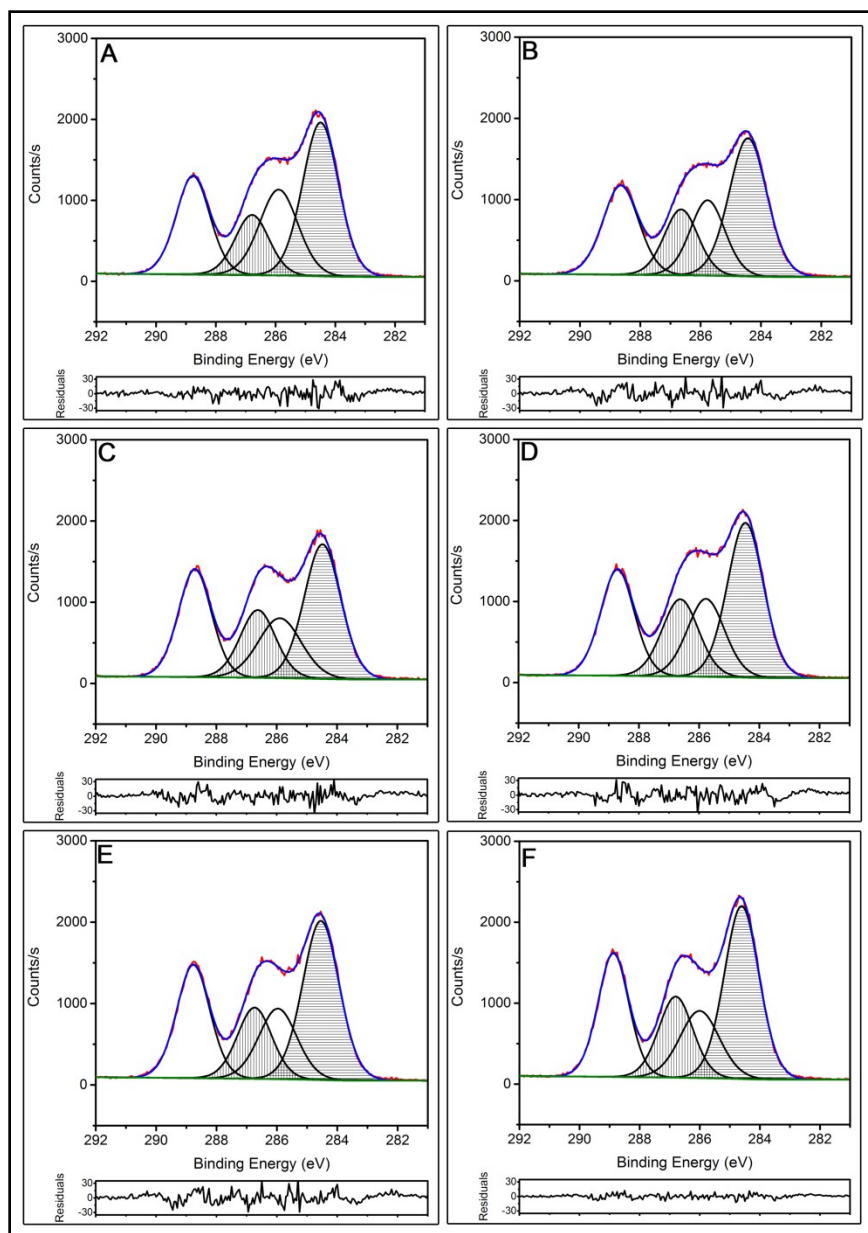
Figure S10 Part A: XPS analysis of uncoated (A) and 0.5-7.5 mg/ml coated PLGA nanoparticles (B-F). The XPS spectra consist of original data (red line), fitted peaks (black line and shaded peaks), cumulative of fitted peaks (blue line) and background used for fitting procedure (green line). Shaded peaks represent C-C bond (284 eV) and –C-O-C- ethoxy bond (286 eV).
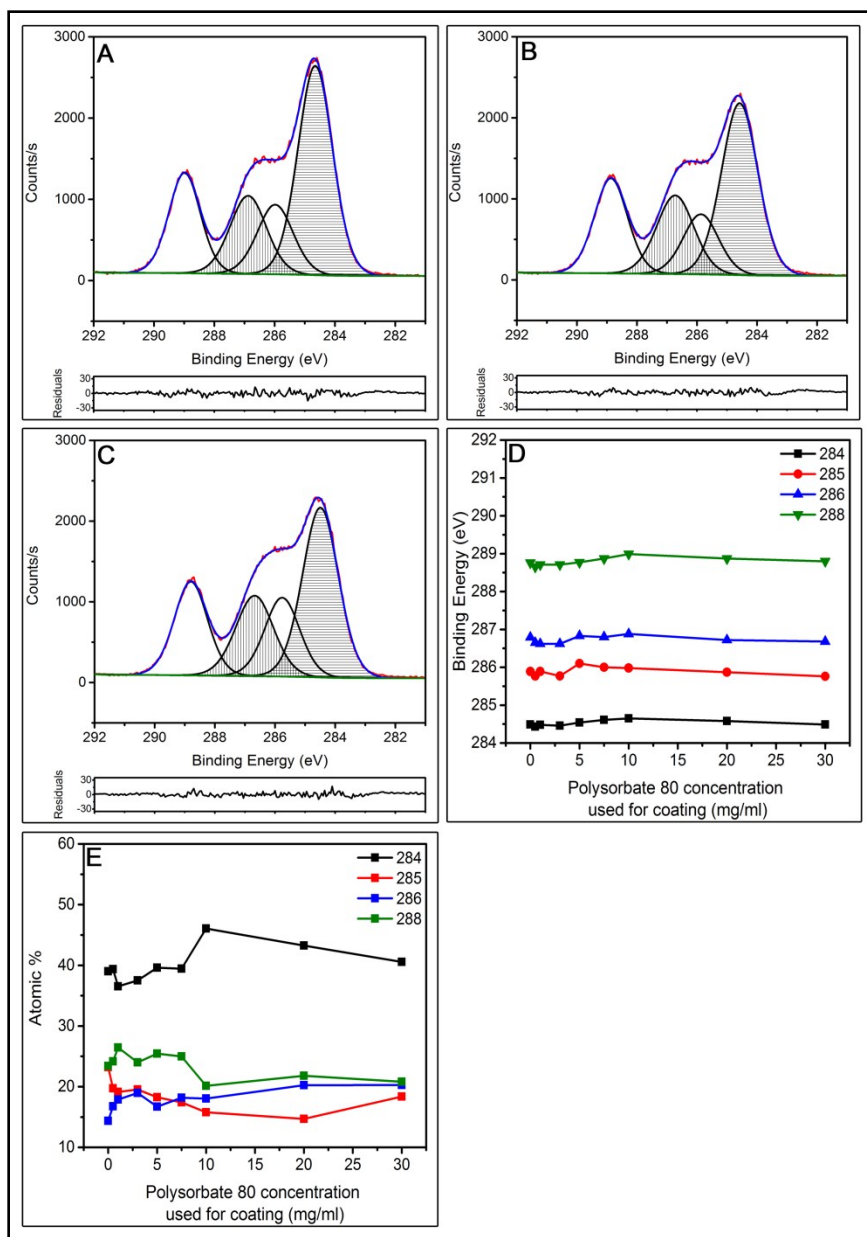
Figure S10 Part B: XPS analysis of 10-30 mg/ml coated PLGA nanoparticles (A-C). The XPS spectra consist of original data (red line), fitted peaks (black line and shaded peaks), cumulative of fitted peaks (blue line) and background used for fitting procedure (green line). Shaded peaks represent C-C bond (284 eV) and –C-O-C- ethoxy bond (286 eV). No shifts were observed in binding energy of any of carbon functionality (D). The atomic % graph showed presence and coverage of polysorbate 80 on PLGA nanoparticle surface (E).
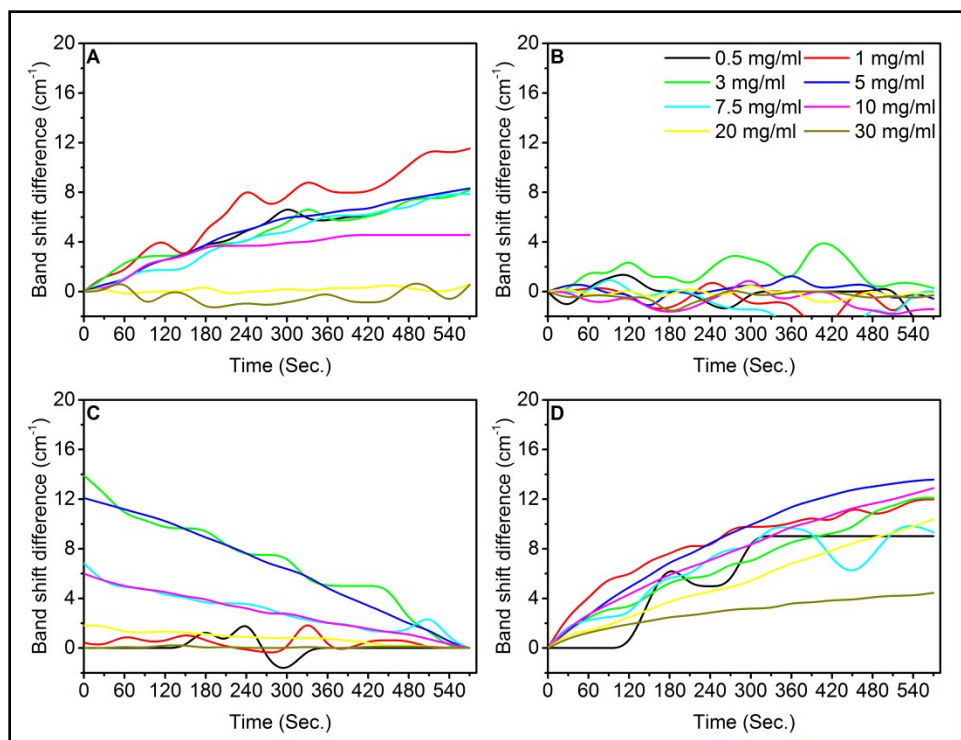
Figure S11: Band shift differences in real-time FTIR analysis of polysorbate 80 in presence of PLGA nanoparticles. (A) Positive shift in symmetric stretching vibrations of acyl chain ($-CH_2$), (B) No shift in asymmetric stretching vibrations of acyl chain, (C) Negative shift in scissoring vibrations of acyl chain, (D) Positive shift in ester ($-C=O$) group vibrations. Positive shift indicates change in peak minima from lower to higher wavenumber, whereas, negative shift indicates change in peak minima from higher to lower wavenumber.
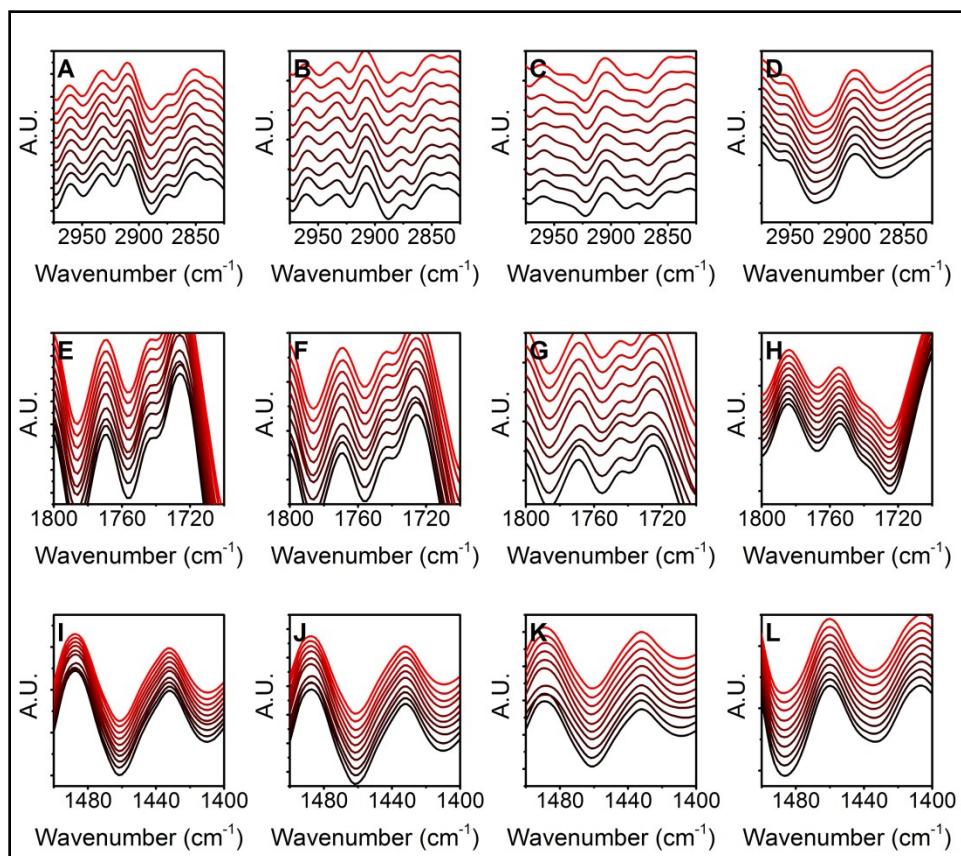
Figure S12 Part A: Real-time FTIR data obtained for polysorbate 80 alone (in absence of PLGA nanoparticles) from repeated measurement mode shows no shifts in stretching vibrations of acyl chain (A-D), ester –C=O group stretching vibrations (E-H), and scissoring vibrations of acyl chain (I-L). Each graph in 1st, 2nd, 3rd and 4th column represents experiment started with 0.5 mg/ml, 1 mg/ml, 3 mg/ml and 5 mg/ml, respectively.
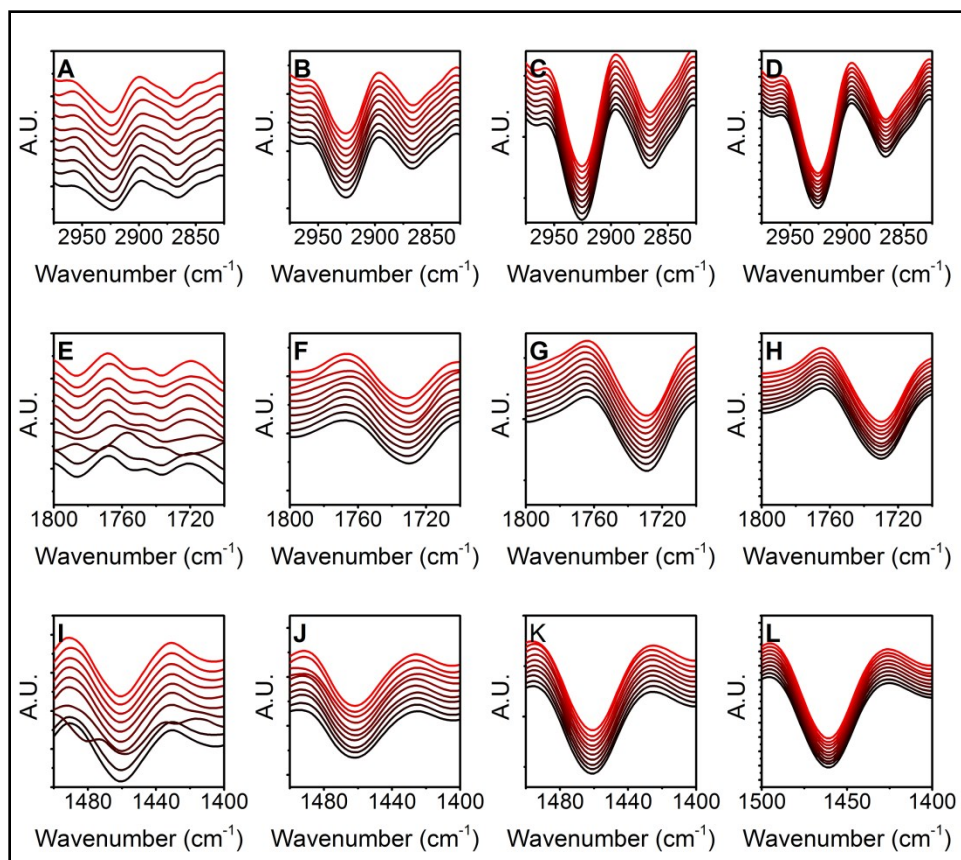
Figure S12 Part B: Real-time FTIR data obtained for polysorbate 80 alone (in absence of PLGA nanoparticles) from repeated measurement mode shows no shifts in stretching vibrations of acyl chain (A-D), ester –C=O group stretching vibrations (E-H), and scissoring vibrations of acyl chain (I-L). Each graph in 1st, 2nd, 3rd and 4th column represents experiment started with 7.5 mg/ml, 10 mg/ml, 20 mg/ml and 30 mg/ml, respectively.
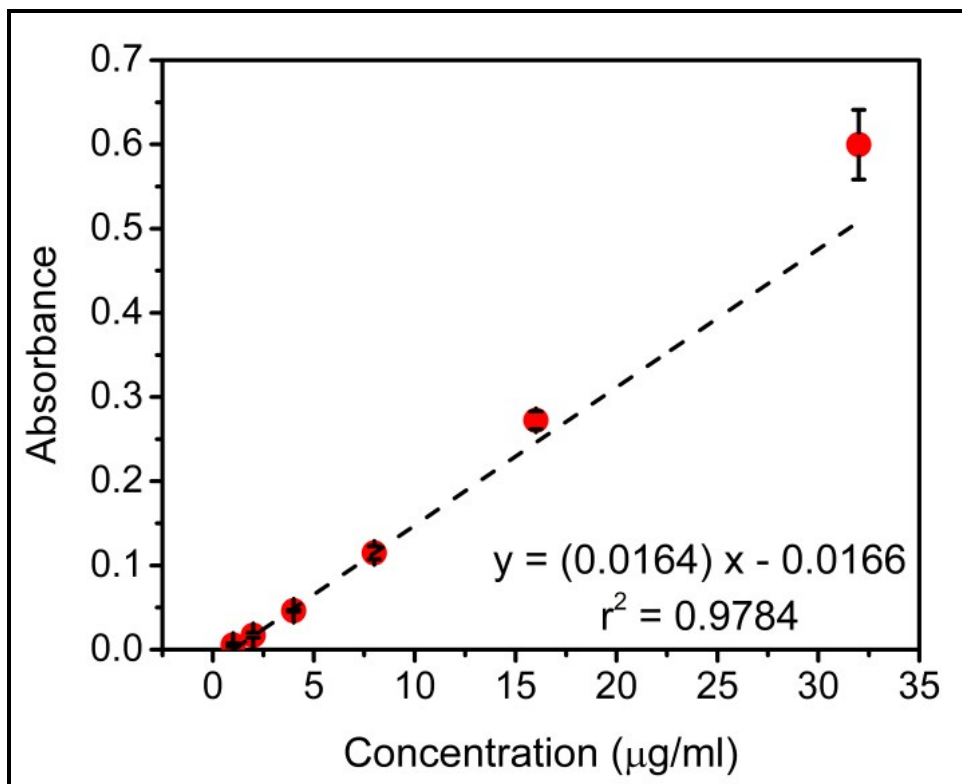
Figure S13: Standard curve for Poly (vinyl) alcohol

REFERENCES:

1. A. V. Delgado, F. Gonzalez-Caballero, R. J. Hunter, L. K. Koopal and J. Lyklema, *J Colloid Interface Sci*, 2007, **309**, 194-224.
2. A. S. Joshi and A. K. Thakur, *Journal of Peptide Science*, 2014, **20**, 630-639.
3. M. M. Zwick, *Journal of Polymer Science Part A-1: Polymer Chemistry*, 1966, **4**, 1642-1644.
4. E. Allemann, J. C. Leroux, R. Gurny and E. Doelker, *Pharm Res*, 1993, **10**, 1732-1737.
5. K. Y. Foo and B. H. Hameed, *Chemical Engineering Journal*, 2010, **156**, 2-10.
6. H. Carstensen, B. W. Müller and R. H. Müller, *International Journal of Pharmaceutics*, 1991, **67**, 29-37.
7. H. Wesemeyer, B. W. Müller and R. H. Müller, *International Journal of Pharmaceutics*, 1993, **89**, 33-40.
8. C. J. Pursell, H. Hartshorn, T. Ward, B. D. Chandler and F. Boccuzzi, *The Journal of Physical Chemistry C*, 2011, **115**, 23880-23892.
9. B. Kronberg and P. Stenius, *Journal of Colloid and Interface Science*, 1984, **102**, 410-417.
10. S. Louguet, A. C. Kumar, N. Guidolin, G. Sigaud, E. Duguet, S. Lecommandoux and C. Schatz, *Langmuir*, 2011, **27**, 12891-12901.
11. M. Danish, R. Hashim, M. N. Mohamad Ibrahim, M. Rafatullah, O. Sulaiman, T. Ahmad, M. Shamsuzzoha and A. Ahmad, *Journal of Chemical & Engineering Data*, 2011, **56**, 3607-3619.
12. V. Bolis, in *Calorimetry and Thermal Methods in Catalysis*, ed. A. Auroux, Springer Berlin Heidelberg, 2013, vol. 154, ch. 1, pp. 3-50.
13. H. Qiu, L. Lv, B.-c. Pan, Q.-j. Zhang, W.-m. Zhang and Q.-x. Zhang, *J. Zhejiang Univ. Sci. A*, 2009, **10**, 716-724.
14. H. A. Spikes, *Langmuir*, 1996, **12**, 4567-4573.